$Na_2MoO_{2-\delta}F_{4+\delta}$ – a perovskite with a unique combination of atomic orderings and octahedral tilts

Hajime Ishikawa,[a] Irene Munaò,[b] Bela E. Bode,[b] Zenji Hiroi[a] and Philip Lightfoot*[b]

Supplementary Information

X-ray Crystallography

Single crystal X-ray diffraction data were measured at 173 K on a Rigaku SCX Mini diffractometer using Mo-Kα radiation (λ =0.71073 Å). Indexing and data processing were performed with Rigaku CrystalClear 2.0 and the structure was solved by direct methods and refined using the SHELX suite incorporated into the WinGX package. Data collection and refinement details are given in Table S1, selected bond lengths, angles and bond valence sums[a] in Table S2. Further details are deposited in CIF format, based on an idealised model with stoichiometry $Na_2MoO_2F_4$: see below for discussion of alternative models considered.

Table S1 Crystal data and refinement details

Empirical formula	$F_4Mo_1Na_2O_2$
Formula weight	249.92
Temperature	173(2) K
Wavelength	0.71075 Å
Crystal system	Monoclinic
Space group, *Z*	*P* $2_1/c$, 4
Unit cell dimensions	a = 5.4800(11) Å
	b = 5.701(7) Å β = 91.316(8) °
	c = 16.319(3) Å
	V = 509.7(6) $Å^3$
D(Calc)	3.257 g/cm^3
μ	2.749 mm^{-1}
F(000)	464
Reflections collected / unique	4853 / 1126 [R(int) = 0.0215]
Data / restraints / parameters	1126 / 0 / 82
Goodness-of-fit on F^2	1.142
Final R indices [I>2σ(I)]	R_1 = 0.0140, wR_2 = 0.0377
R indices (all data)	R_1 = 0.0153, wR_2 = 0.0381
Largest diff. peak and hole	0.390 and -0.526 e $Å^{-3}$

Table S2 Selected bond lengths (Å), angles (deg) and bond valence sums (valence units)

		Bond	Bond valence		Bond angle
Mo1	O1	1.684(2)	1.827	Mo1-O1-Na2	149.48(9)
	O2	1.727(1)	1.627	Mo1-O2-Na2	151.09(8)
	F4	1.916(2)	0.751	Mo1-F1-Na2	146.46(6)
	F3	1.960(2)	0.667	Mo1-F2-Na2	134.44(6)
	F2	2.050(1)	0.523	Mo1-F3-Na2	137.73(6)
	F1	2.121(1)	0.431	Mo1-F4-Na2	141.10(6)
Na1	O2	2.716(2)	0.084		
	O2	3.163(3)	0.025		
	F1	2.302(1)	0.185		
	F1	2.349(3)	0.163		
	F1	3.321(3)	0.011		
	F2	2.306(2)	0.183		
	F2	2.496(2)	0.109		
	F3	2.364(2)	0.156		
	F3	2.554(2)	0.093		
	F4	2.562(2)	0.091		
Na2	O1	2.349(2)	0.227		
	O2	2.364(3)	0.218		
	F1	2.353(1)	0.161		
	F2	2.227(2)	0.226		
	F3	2.309(2)	0.181		
	F4	2.245(2)	0.215		

[Based on idealised stoichiometry $Na_2MoO_2F_4$ with no anti-site O/F defects]

Bond Valence Sums: Mo1 5.83, Na1 1.10, Na2 1.22, O1 2.05, O2 1.94, F1 0.95, F2 1.04, F3 1.10, F4 1.06

Estimation of the true stoichiometry

Although the idealised structural model proposed here provides an extremely good fit to the single crystal data, the blue sample colour clearly suggests some degree of reduction to Mo^{5+}. In order to probe this, several analytical techniques were considered, *viz.* (i) EPR (ii) magnetization measurement (iii) direct chemical titration. Unfortunately, due to the presence of MoO_2 contamination, a suitable sample for direct and reliable chemical analysis was not obtained. Reduction to Mo^{5+} might be correlated with Na or Mo off-stiochiometry or O/F off-stoichiometry.

Single crystal XRD

First of all, several test models of the single crystal data were analysed. These models adapt the final, idealised model presented in the CIF (R_1 = 0.0140, wR_2 = 0.0377), with the addition of specific variables, as follows:

1. Free refinement of Mo occupancy. This resulted in a refined value Occ(Mo) = 0.973(3), and very slightly reduced R-values ([I>2σ(I)] : R_1 = 0.0139, wR_2 = 0.0345).
2. Free refinement of occupancies of Na1 and Na2: refined values Occ(Na1) = 1.005(5), Occ(Na2) 1.028(6); R_1 = 0.0141, wR_2 = 0.0377.
3. Inclusion of an interstitial Na atom (fixed U_{iso} = 0.01 Å^2) at the ideal position (¼, ¼, ½) of the A-site vacancy: refined Occ = 0.005(3).

4. Free, simultaneous refinement of occupancies for O1, O2 and F1-F4, with atoms types fixed as O and F, respectively: Refined occupancy values (in order O1 – F4) 1.054(7), 1.070(5), 1.036(5), 1.036(4), 1.030(4), 1.020(4); R_1 = 0.0132, wR_2 = 0.0327.
5. Refinement of full-occupancy anti-site anion defects of the type O→F or F→ O. For example, O1 being refined freely as 100% F (R_1 = 0.0173, wR_2 = 0.0459); O2 being refined freely as 100% F (R_1 = 0.0167, wR_2 = 0.0455); F1 being refined freely as 100% F (R_1 = 0.0207, wR_2 = 0.0625); in each case the atomic displacement parameters became unreasonable, and in the case of F→ O substitution non-positive definite.
6. Refinement of sites O1 and O2 as mixed O/F occupancy, assuming full occupancy of both sites, and applying EXYZ and EADP constraints to the mixed O/F atoms. Refined occupancies O1 = 0.80(3) O / 0.20(3) F; O2 = 0.72(3) O / 0.28(3) F; F R_1 = 0.0137, wR_2 = 0.0355.

From test refinement 1 we conclude that there is unlikely to be any Mo deficiency and/or Na substitution at the Mo site. Instead, the reduced occupancy is most likely an artefact of employing 'neutral atom' scattering factors, whereas the Mo-X bonds are probably slightly 'ionic'.

From test refinements 2 and 3 there is no evidence for Na deficiency at either Na1 or Na2, nor any occupancy at the vacant A-site.

From test refinement 4 we conclude that there is some *slight* evidence for O deficiency/ F substitution at both sites O1 and O2; the occupancies for both O sites being significantly larger than those at the F sites. We note also that the refined values of the F sites also support the premise that the use of neutral atom scattering factors highlights that there is some clear indication of partial 'ionic' character of the F sites. Ionic character could, of course, also influence the O site occupancies, so the suggestion of F occupancy at the O sites is tentative from these refinement models.

From test refinement 5 we conclude that the present, high-quality single crystal XRD is a perfectly reliable means of distinguishing O and F atoms, *if full substitution only* is considered. There is *very clearly* a difference in the net electron density at the F (versus O) sites.
In the light of test refinements 4 and 5, there is no evidence for F-deficiency or O-substitution at any of the four F sites. Anion ordering is therefore complete, within the limitations of the perceived stoichiometry.

Taking the anion occupancies derived from test refinement 6 at face value leads to an overall stoichiometry $Na_2MoO_{2-\delta}F_{4+\delta}$, δ = 0.48; however in the light of the over-estimation of F occupancies in test refinement 4 (an artefact of these sites being significantly 'ionic') we suggest that the true value of δ is considerably smaller than this, based purely on the crystallographic data. Note that test refinement 6 makes relatively little difference to the R-factors compared to test 4, which clearly contains artefacts.

The overall conclusion here is that evidence for *some* degree of off-stoichiometry on the anion sublattice is discernible directly from the single crystal XRD, but precise and reliable quantification is problematic.

Other methods were trialled, based on direct detection of reduced Mo species (see below).

Powder X-ray diffraction data

PXRD data were collected on a Stoe STADI/P diffractometer in transmission mode (0.3 mm glass capillary) using $CuK_{\alpha 1}$ radiation. Rietveld refinement (GSAS) is shown in Figure S1.

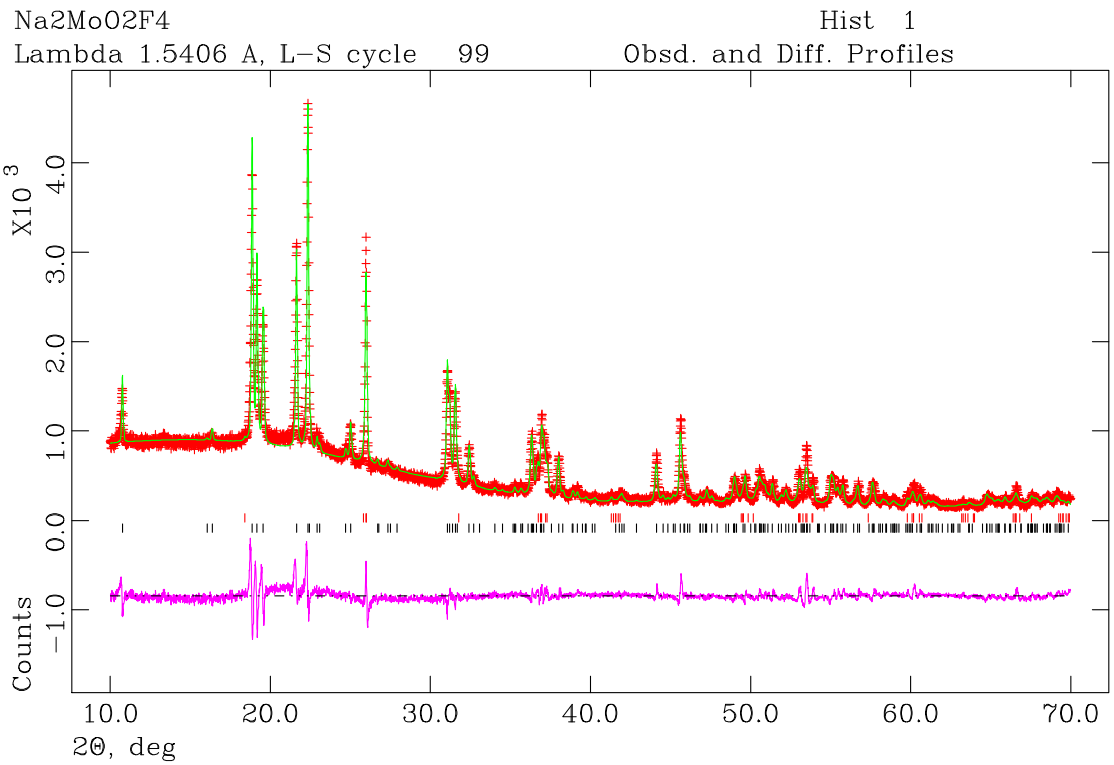

Figure S1. Rietveld refinement of the powder X-ray diffraction data. A phase distribution of ~87% $Na_2MoO_2F_4$ and ~13% monoclinic MoO_2 (ICSD-80830[b]) was derived. For the sake of phase identification only, the structural parameters were fixed from the single crystal models, and lattice parameters, peaks shapes and phase fractions only were refined.

Electron paramagnetic resonance

EPR spectra were obtained with a Bruker EMX 10/12 spectrometer and an SHQE resonator operating at ~9.36 GHz with 100 kHz modulation. Samples were contained in 4 mm OD quartz tubes (Wilmad lab-glass) sealed with rubber septa (Sigma-Aldrich). The spectrum was recorded using a 200 mT field sweep centred at 355 mT with 2048 points resolution, a time constant and conversion time of 40.96 ms each, a modulation amplitude of 0.1 mT and a microwave frequency of 9.3600 GHz. The complicated line pattern is likely to be due to not completely resolved ^{95,97}Mo and ^{19}F-hyperfine interactions in close resemblance of the frozen solution EPR spectrum[c] of $[MoOF_5]^{2-}$. This method was not deemed suitable for quantitative analysis, due to the lack of a reliable paramagnetic Mo^{5+} standard.

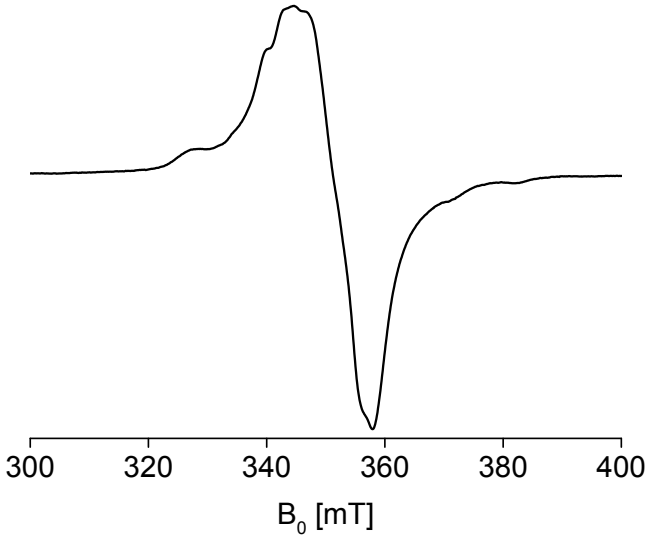

Figure S2. Room temperature continuous wave X-Band EPR of a solid sample of $Na_2MoO_{2-\delta}F_{4+\delta}$.

Magnetisation

Magnetic susceptibility at 2-300 K (Figure S3) and magnetization curve at 2 K (inset) were measured by using a SQUID magnetometer (MPMS3, Quantum Design). Magnetic susceptibility increases drastically at low temperatures as typically observed for localised free spins. We assume that the main contribution comes from Mo^{5+} ions with localised spin-1/2 in $Na_2MoO_{2-\delta}F_{4+\delta}$, which comprise 87% of the powder sample (from the Rietveld analysis); the minor phase of MoO_2 is a paramagnetic metal which shows a small and temperature independent susceptibility[d]. The data are well fitted by Curie's law with a constant χ_0, $\chi = \chi_0 + C/T$, where χ_0 = 2.34(5) $\times 10^{-5}$ cm^3 mol-Mo^{-1} and C = 0.0301(2) cm^3 K mol-Mo^{-1} (red line in Figure). The Curie Constant corresponds to 8.0% of the 0.375 cm^3 K mol^{-1} expected for spin-1/2. The magnetization curve at 2 K can be reproduced by a Brillouin function which saturates toward 0.0746(6) μ_B mol-Mo^{-1} (red line in the inset). These results suggest that approximately 8% of Mo ions in $Na_2MoO_{2-\delta}F_{4+\delta}$ exist as Mo^{5+} ions, i.e. $\delta \sim 0.08$.

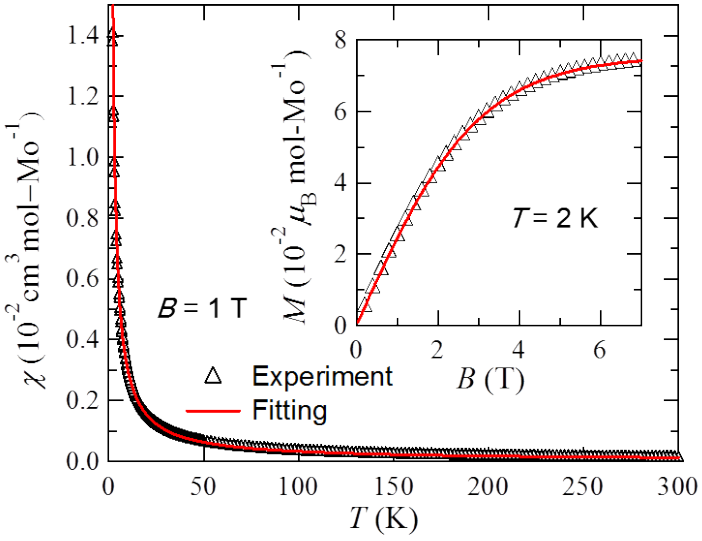

Figure S3. Magnetic susceptibility of the powder sample of $Na_2MoO_{2-\delta}F_{4+\delta}$ at 2-300 K, measured in 1 T, and magnetization curve at 2 K (inset). Red lines are the fittings described in the text.

Distortion Mode Analysis

The on-line program ISODISTORT[e] was used to decompose the structure into its constituent normal modes. Full details of the output from this analysis are provided in supplementary file ISODISTORT.txt.

In order to account for A-site ordering a dummy atom was included at the vacant A-site (ideal position (¼, ¼, ½)). There are therefore 27 variable atomic coordinates plus 3 null variables for the vacancy, which can be re-cast as 30 displacive modes. Of these, the ones with the largest amplitudes are the R_4^+ and T_4 octahedral tilt modes (respectively the out-of-phase tilts around the pseudo-cubic *a* and *b* axes and the AACC tilt around *c*), and the oxygen displacement modes described by *irreps* R_1^+, Δ_5 and X_3^-. Δ_5 and X_3^- act to distort the octahedra and R_1^+ is a symmetric octahedral 'breathing' mode, which modifies the relative sizes of MoX_6 and $Na(2)X_6$ octahedra. There is also a significant Na(1) displacement mode: this is the Δ_5 mode, which is an antiferrodistortive displacement along the *b*-axis, which is also significant in antiferroelectric $NaNbO_3$. In addition there are 10 possible occupancy modes, of which only 6 are active: R_1^+ describes the Na(2)/Mo ordering on the B-site; X_3^- describes the layered ordering of Na(1)/Vac on the A-site, and also the 'apical' O(1)/F(1) ordering; M_5^- describes the 'in-plane' O/F ordering (the Γ modes are normalisation modes only).

References

a. N. E. Brese and M. O'Keeffe, *Acta Crystallogr*., 1991, **B47**, 192
b. A. A. Bolzan, B. J. Kennedy and C. J. Howard, *Aust. J. Chem*., 1995, **48**, 1473.
c. C. Balagopalakrishna, J. T. Kimbrough, and T. D. Westmoreland *Inorg. Chem.* 1996**, 35**, 7758.
d. E. Røst, J. Am. Chem. Soc. 1959, **81**, 3843.
e. B. J. Campbell, H. T. Stokes, D. E. Tanner and D. M. Hatch, *J. Appl. Crystallogr*., 2006, **39**, 607